MATERIALS CHEMISTRY FRONTIERS

RESEARCH ARTICLE

View Article Online
View Journal | View Issue

Cite this: *Mater. Chem. Front.*, 2017, **1**, 1310

A bifunctional covalent organic framework as an efficient platform for cascade catalysis†

Qi Sun, Briana Aguila and Shengqian Ma*

Received 15th December 2016,
Accepted 22nd January 2017

DOI: 10.1039/c6qm00363j

rsc.li/frontiers-materials

Published on 23 January 2017. Downloaded on 28/06/2017 16:16:36.

A bifunctional covalent organic framework (COF) has been illustrated in the context of partial metalation of a highly porous and chemically robust pyridine containing COF (COF-TpPa-Py) with Pd species and by taking advantage of the base catalytic behavior of pyridine. The resultant bifunctionalized COF exhibits excellent performance in catalyzing one-pot cascade aerobic oxidation–Knoevenagel condensation reactions, outperforming the corresponding homogeneous and porous organic polymer based catalytic systems, thereby opening a new avenue for multifunctional COFs as a promising platform for heterogeneous cascade catalysis.

Introduction

The development of cascade reaction processes that incorporate several reactions to give the final product in one operation has recently emerged as a promising field for advancing modern and sustainable chemistry. Given that the consecutive reaction steps are performed in one pot, costly intermediate separations and purification processes will be avoided, thus offering enormous economic advantages.[1] In most cases, a multistep chemical process involves several active components such as a metal, ligand, base, and other cofactors.[2] Efforts are thus being made to integrate different catalytically active sites within a single and recyclable material to facilitate one-pot cascade catalysis.[3,4] It has been well-documented that careful positioning of these individual functions on a solid support provides a promising strategy for improving catalytic performance by tailoring synergistic interactions, in a way reminiscent of enzymatic catalysis.[5] In this context, a material which enables precise control over chemical functionality, density, and spatial arrangement of the active sites is highly desirable.

Covalent organic frameworks (COFs)[6] as a new class of crystalline materials, with highly ordered organic building blocks and discrete nanopores, have spurred great interest due to their potential applications pertaining to environmental remediation,[7] catalysis,[8] proton conduction,[9] and many more.[10] A distinct feature of COFs is that total control over their structure and properties can be achieved through careful selection of the building units prior to synthesis. This unique feature is very attractive to design multifunctional catalysts, considering that the functionality, density, and spatial arrangement of the active sites can be precisely managed. In particular, two dimensional (2D) COFs exhibit unique architectures wherein the monomers that make up their 2D layers stack almost perfectly into infinite 1D columns that are ideal for docking catalysts through the modification of the building blocks, due to the potentially improved accessibility of active sites and mass transport. COFs are thus expected to serve as an auspicious platform for integrating multiple components to bring into effect cascade catalysis.

Considering the attractive catalytically related functionality of pyridine, which can act as a base catalyst and a nitrogen donor to bind metal species, in this contribution, a chemically stable COF bearing pyridine (COF-TpPa-Py) was chosen to demonstrate a proof-of-concept for the utilization of COFs as a promising platform for cascade catalysis. Representatively, after partial metalation of the pyridine groups in COF-TpPa-Py with $Pd(OAc)_2$, the resultant catalyst (Pd/COF-TpPa-Py) was found to be highly active, selective, and recyclable for the one-pot cascade synthesis involving Pd-catalyzed aerobic oxidation of alcohols to aldehydes and base-catalyzed Knoevenagel condensation with the remaining free pyridine groups (Scheme 1). Notably, the COF catalyst outperforms the corresponding homogeneous analogues and the porous organic polymer based catalytic systems in terms of turnover frequency. The site-isolation manner in conjunction with the accessibility of the active sites in Pd/COF-TpPa-Py accounts for the observed excellent performance. Our work thereby sheds light on the great potential of COFs for the design of heterogeneous cascade catalysis.

Experimental

Materials

Solvents were purified according to standard laboratory methods. Other commercially available reagents were purchased in high purity and used without further purification.

Department of Chemistry, University of South Florida, 4202 E. Fowler Avenue, Tampa, FL 33620, USA. E-mail: sqma@usf.edu

† Electronic supplementary information (ESI) available. See DOI: 10.1039/c6qm00363j

 This journal is © The Royal Society of Chemistry and the Chinese Chemical Society 2017

Published on 23 January 2017. Downloaded on 28/06/2017 16:16:36.

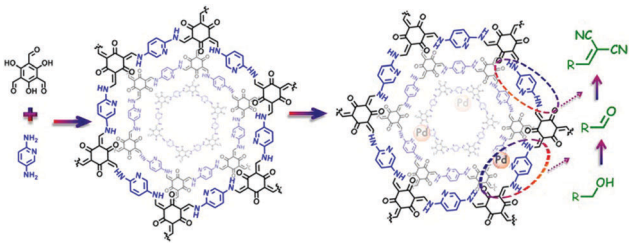

Scheme 1 Schematic of Pd/COF-TpPa-Py synthesis and one-pot cascade aerobic oxidation–Knoevenagel condensation reactions. The Pd/pyridine complex catalyzed oxidation of alcohols to aldehydes and the free pyridine group catalyzed Knoevenagel condensation.

Catalyst synthesis

Synthesis of COF-TpPa-Py. A Pyrex tube measuring o.d. × i.d. = 9.5 × 7.5 mm^2 was charged with triformylphloroglucinol (21 mg, 0.10 mmol) and 2,5-diaminopyridine (16.3 mg, 0.15 mmol) in 1.1 mL of a 5 : 5 : 1/v : v : v solution of 1,4-dioxane : mesitylene : 6 M aqueous acetic acid. The tube was flash frozen at 77 K (liquid N_2 bath), evacuated and flame sealed. Upon sealing the length of the tube was reduced to *ca.* 15 cm. The reaction mixture was heated at 120 °C for 3 days to afford a reddish brown precipitate which was isolated by filtration and washed with anhydrous THF using soxhlet extraction for 3 days. The product was dried under vacuum to afford COF-TpPa-Py (27.9 mg, 75%).

Synthesis of *x* Pd/COF-TpPa-Py (*x* stands for the loading amount of Pd species). As a typical run, the mixture of $Pd(OAc)_2$ (60 mg) and COF-TpPa-Py (500 mg) in toluene (20 mL) was stirred at room temperature overnight. After that, the solid was filtered, washed with excess toluene and acetone, and dried under vacuum to afford Pd/COF-TpPa-Py. ICP-OES results reveal that the Pd loading amount in Pd/COF-TpPa-Py was 4.1 wt%.

Synthesis of POP-Py[11]. 1.42 g of divinylbenzene and 0.58 g of 4-vinylpyridine were dissolved in 20 mL of THF, followed by the addition of 50 mg of AIBN. The mixture was transferred into an autoclave at 100 °C for 24 h. The title polymer was obtained after being washed with THF and evaporated under vacuum.

Synthesis of Pd/POP-py. A mixture of $Pd(OAc)_2$ (60 mg) and POP-Py (500 mg) in toluene (50 mL) was stirred at room temperature overnight. After that, the solid was filtered, washed with excess toluene and acetone, and dried under vacuum to afford Pd/POP-Py. ICP-OES results reveal that the Pd loading amount in Pd/POP-Py was 3.9 wt%.

Catalytic tests

The one-pot cascade aerobic oxidation–Knoevenagel condensation reactions were carried out in a 50 mL Schlenk flask with a magnetic stirrer. In a typical run, alcohol (1 mmol), the catalyst listed in Table 1, and toluene (10 mL) were transferred into the reactor. After being evacuated, the system was purged with O_2 using a balloon. The tube was placed in a preheated oil bath and stirred for the desired time. After the reaction progressed for the desired period of time, the oxygen balloon was removed, and then malononitrile (1.05 mmol) was charged into the reaction system rapidly. The mixture was left at 80 °C for an additional time period. The conversion and the yield of the products were analyzed by ^1H NMR.

Table 1 Catalytic performance of the cascade oxidation–Knoevenagel reaction from benzyl alcohol to benzylidene malononitrile over various catalysts[a]

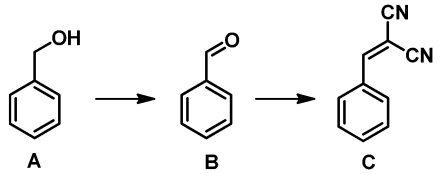

Entry	Catalyst	Conv. (%) A	Yield (%) B	Yield (%) C
1[b]	Pd/COF-TpPa-Py	98	Trace	98
2[c]	COF-TpPa-Py	Trace	Trace	Trace
3[d]	$Pd(OAc)_2$	5	5	Trace
4[e]	$Pd(OAc)_2$ + pyridine	79	Trace	79
5[f]	Pd/POP-Py	72	4	67

[a] Reaction conditions: a mixture of benzyl alcohol (1 mmol), toluene (10 mL), and catalyst was stirred at 80 °C under O_2 (1 atm) for 4 h and then malononitrile (1.05 mmol) was introduced and the reaction continued for another 1.5 h. [b] Pd/COF-TpPa-Py (65 mg containing 0.025 mmol Pd and 0.2 mmol pyridine moieties). [c] COF-TpPa-Py (65 mg). [d] $Pd(OAc)_2$ (5.6 mg, 0.025 mmol Pd). [e] $Pd(OAc)_2$ (5.6 mg) and pyridine (15.8 mg, 0.2 mmol). [f] Pd/POP-Py (68 mg containing 0.025 mmol Pd and 0.18 mmol pyridine moieties).

For each catalyst recycling, the catalysts were separated by centrifugation under N_2, washed with degassed toluene, and used directly for the next run.

Characterization

The gas adsorption isotherms were collected on an ASAP 2020 surface area analyzer. The N_2 sorption isotherms were measured at 77 K using a liquid N_2 bath. Powder X-ray diffraction (PXRD) data were collected on a Bruker AXS D8 Advance A25 Powder X-ray diffractometer (40 kV, 40 mA) using Cu Kα (λ = 1.5406 Å) radiation. Scanning electron microscopy (SEM) images were collected using a Hitachi SU 8010. IR spectra were recorded on a Nicolet Impact 410 FTIR spectrometer. ICP-OES was performed on a Perkin-Elmer Elan DRC II Quadrupole. X-ray photoelectron spectroscopy (XPS) was performed on a Thermo ESCALAB 250 with Al Kα irradiation at θ = 90° for the X-ray source, and the binding energies were calibrated using the C1s peak at 284.9 eV. ^1H NMR spectra were recorded on a Bruker Avance-400 (400 MHz) spectrometer. Chemical shifts are expressed in ppm downfield from tetramethylsilane (TMS) at δ = 0 ppm, and J values are given in Hz. The ^{13}C (100.5 MHz) cross-polarization magic-angle spinning (CP-MAS) solid-state NMR experiment was recorded on a Varian infinity plus 400 spectrometer equipped with a magic-angle spin probe in a 4 mm ZrO_2 rotor.

Results and discussion

With the aim of optimizing the porosity and crystallinity of COF-TpPa-Py (Fig. 1a), we screened the synthetic conditions by varying the solvent combination/ratio and catalyst loading. Under optimal synthetic conditions, reacting 1,4-dioxane, mesitylene, and 6 M acetic acid in a 5 : 5 : 1 (v : v : v) ratio at 120 °C for 3 days,

Published on 23 January 2017. Downloaded on 28/06/2017 16:16:36.

we obtained COF-TpPa-Py as a reddish brown microcrystalline solid in a yield of about 75%. The Fourier transform infrared (FT-IR) spectrum of COF-TpPa-Py indicated the complete consumption of the reactants as evidenced by the disappearance of the characteristic N–H stretching bands (3286–3372 cm^{-1}) of the free diamine and aldehydic –C═O (1640 cm^{-1}). Moreover, the absence of C═N stretching peaks at around 1620 cm^{-1} and the appearance of a new C═C peak at 1570 cm^{-1} verified the transformation of the enol into a keto tautomer (Fig. S1, ESI†).[12] Solid-state ^{13}C NMR spectroscopy confirmed the existence of the keto tautomer supported by the presence of the peak at ~183 ppm, which is attributed to the keto (–C═O) group (Fig. 1b). The detailed assignment of these peaks is given in Fig. S2 (ESI†). The PXRD pattern of COF-TpPa-Py showed an intense reflection at 4.6° corresponding to the (100) plane (Fig. 1c). The reflections at 7.8°, 9.5°, 12.1°, and ~27° are attributed to the (110), (200), (210), and (001) planes, respectively. This is in agreement with the theoretical prediction of an AA stacking arrangement. The permanent porosity of COF-TpPa-Py was determined by measuring nitrogen adsorption at 77 K. As shown in Fig. 1d, COF-TpPa-Py displayed a type I isotherm with a sharp uptake in the low relative pressure region ($P/P_0 < 0.1$), which is characteristic of microporous materials. The Brunauer–Emmett–Teller surface area and the total pore volume of COF-TpPa-Py were calculated to be 1019 $m^2\ g^{-1}$ and 0.56 $cm^3\ g^{-1}$, respectively. DFT fitting of the adsorption branches showed pore size distributions mainly at 1.5 nm, in good agreement with that of the proposed model (Fig. S3, ESI†). The framework of COF-TpPa-Py is stable under a wide range of conditions as demonstrated by its well-retained crystallinity after soaking it in a variety of solvents as well as in both acid (2 M HCl) and base (2 M NaOH) aqueous solutions (Fig. S4, ESI†). In addition, thermogravimetric analysis (TGA) revealed that COF-TpPa-Py exhibited no weight loss under N_2 up to 400 °C, indicating its excellent thermal stability (Fig. S5, ESI†).

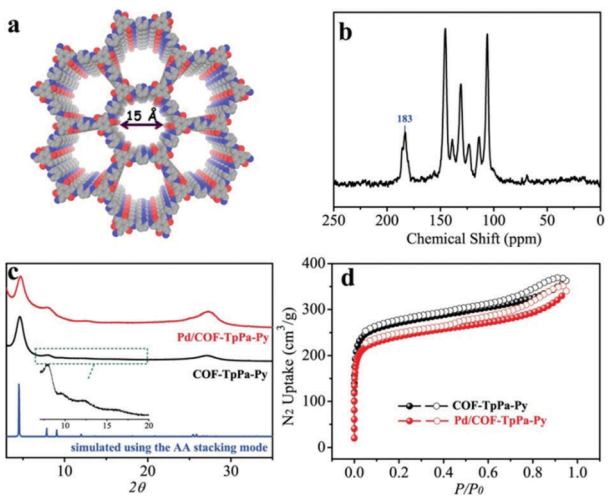

Fig. 1 (a) View of the slipped AA stacking structure of COF-TpPa-Py (O, red; N, blue; C, grey), (b) the ^{13}C MAS NMR spectrum of COF-TpPa-Py, (c) simulated and experimental PXRD patterns, and (d) N_2 sorption isotherms collected at 77 K.

With a porous and crystalline pyridine functionalized framework available, we proceeded to synthesize COF-TpPa-Py into heterogeneous multifunctional catalysts for cascade reactions. By virtue of the pyridine-related base catalytic behavior and its strong coordination ability to metal species, it is highly promising to develop a multifunctional catalyst to be used for a cascade process involving a redox step followed by base catalysis. Given that a Pd/pyridine catalytic system shows excellent activity for aerobic oxidation of alcohols,[13] we envision that partially metalated COF-TpPa-Py with Pd species, the resultant Pd/COF-TpPa-Py catalyst bearing two types of active sites, holds great promise for application in one-pot cascade catalysis.

With these aspects in mind, we treated COF-TpPa-Py with $Pd(OAc)_2$ to afford Pd/COF-TpPa-Py and investigated its catalytic performance in the synthesis of α,β-unsaturated dinitriles from alcohols, which are very important chemical intermediates in the pharmaceutical industry. Given that the catalytic component in the resultant catalysts changes along with the variation of Pd loading amounts, we adjusted the Pd amount on COF-TpPa-Py to achieve the optimal trade-off for the cascade reactions. Three catalysts with Pd loadings of 2.0 wt%, 4.1 wt%, and 7.5 wt%, as revealed by ICP-OES analysis, were synthesized, which were denoted as 2.0 wt% Pd/COF-TpPa-Py, 4.1 wt% Pd/COF-TpPa-Py, and 7.5 wt% Pd/COF-TpPa-Py, respectively. The 4.1 wt% Pd/COF-TpPa-Py (hereafter denoted as Pd/COF-TpPa-Py) was chosen as a representative sample for thorough investigation. The PXRD pattern of the obtained metalated material exhibited a diffraction pattern comparable to that of COF-TpPa-Py with an intensive reflection at 4.7° (Fig. 1c). Nitrogen sorption measurements were conducted to verify pore accessibility after partial metalation (Fig. 1d). The BET surface area of Pd/COF-TpPa-Py was determined to be 902 $m^2\ g^{-1}$, thus indicating the retention of porosity. Correspondingly, the pore size distribution of Pd/COF-TpPa-Py concentrates at 13 Å and 15 Å (Fig. S6, ESI†). Scanning electron microscopy (SEM) images of Pd/COF-TpPa-Py showed a rough surface composed of thin rods. This is similar to the observed morphology of COF-TpPa-Py (Fig. S7, ESI†). Based on the above we can conclude that no distinct structural changes occurred during the introduction of $Pd(OAc)_2$. To investigate the coordination of Pd species with COF-TpPa-Py, Fourier transform infrared spectroscopy (FT-IR) and X-ray photoelectron spectroscopy (XPS) were performed (Fig. 2). The appearance of a new peak at around 690 cm^{-1} in the IR spectrum of Pd/COF-TpPa-Py, which was also observed in the complex of Pd/pyridine (not present in the spectra of both $Pd(OAc)_2$ and pyridine), indicates that complexes formed between Pd species and the pyridine moieties in COF-TpPa-Py (Fig. S8, ESI†). In addition, the XPS study of COF-TpPa-Py showed two different types of N species: one at 398.5 eV for the pyridinic ($-C_5H_3N$) nitrogen and the other at 400.2 eV, ascribed to the free secondary amine (–NH). The ratio of these N species is approximately 1 : 2, which is in good agreement with the theoretical composition. In contrast, the ratio of free pyridinic nitrogen in Pd/COF-TpPa-Py is obviously lower than COF-TpPa-Py as demonstrated by the decreased area ratio (0.5 to 0.36) of N species at around 398.5 eV, suggesting that part of the pyridinic nitrogens coordinate with the Pd species,

 This journal is © The Royal Society of Chemistry and the Chinese Chemical Society 2017

Published on 23 January 2017. Downloaded on 28/06/2017 16:16:36.

thereby shifting to a higher binding energy.[14] Meanwhile, Pd/COF-TpPa-Py demonstrated the binding energies of Pd $3d_{3/2}$ and Pd $3d_{5/2}$ at 342.9 and 337.6 eV, respectively, which are significantly lower than those of $Pd(OAc)_2$ (343.8 and 338.6 eV, respectively).[15] These results indicate that strong interactions exist between the Pd species and pyridine moieties in the Pd/COF-TpPa-Py. High angle annular dark field scanning transmission electron microscopy (HADDF-STEM) and EDX mapping results revealed that Pd species are homogeneously distributed throughout the material and no aggregated Pd nanoparticles are observed (Fig. S9, ESI†).

Given the accessibility together with the well-defined and arranged active sites, we set out to evaluate the performance of bifunctional COF materials as a bifunctional solid catalyst in the context of a metal-base catalyzed one pot cascade reaction involving the aerobic oxidation of alcohols and the subsequent Knoevenagel condensation. To achieve the optimal catalytic activities, we first investigated the relationship between the cascade catalytic performance and the ratio of the two types of active sites in the Pd metalated COF-TpPa-Py by comparison of the turnover frequency (TOF) values for each individual step. For the oxidation step, 2.0 wt% Pd/COF-TpPa-Py, Pd/COF-TpPa-Py, and 7.5 wt% Pd/COF-TpPa-Py gave TOF values of 16.1, 15.7, and 11.4 h^{-1}, respectively, after 1 h. For ease of comparison, benzaldehyde was used as the reagent to test the efficiency of Knoevenagel condensation over various catalysts. The 2.0 wt% Pd/COF-TpPa-Py, Pd/COF-TpPa-Py, and 7.5 wt% Pd/COF-TpPa-Py afforded TOF values of 2.1, 2.5, and 2.6 h^{-1}, respectively, after 30 min. In view of the TOF values for the two steps, Pd/COF-TpPa-Py was chosen for further detailed studies.

Next, to illustrate the advantages of the bifunctional COF catalytic systems in the one-pot synthesis, a set of control experiments including the homogeneous $Pd(OAc)_2$/pyridine catalyst and a $Pd(OAc)_2$ metalated pyridine-containing porous organic polymer (Pd/POP-py), which was synthesized by copolymerization of divinylbenzene and 4-vinylpyridine, were conducted. In a typical run, the reactions were carried out in a Schlenk tube purged with atmospheric O_2 using benzyl alcohol and malononitrile as reactants and toluene as the solvent in the presence of catalysts at 80 °C, with the results listed in Table 1. Benzaldehyde was produced as an intermediate, and benzylidene malononitrile was the objective product in all cases. Remarkably, Pd/COF-TpPa-Py showed exceptional catalytic activity, giving rise to a benzylidene malononitrile yield as high as 98%, which outperformed all other catalytic systems tested under the same conditions. Considering that COF-TpPa-Py did not convert benzyl alcohol (Table 1, entry 2) and $Pd(OAc)_2$ exhibited poor activity, affording benzaldehyde in a 5% yield with a negligible amount of benzylidene malononitrile, the excellent performance of Pd/COF-TpPa-Py thereby should be attributed to the combined contributions from the COF-TpPa-Py and Pd species. It is known that the presence of a base, such as pyridine, is beneficial to promote the Pd-catalyzed oxidation and additionally the base is the active species for the Knoevenagel condensation. Therefore, Pd/COF-TpPa-Py with these features can facilitate the cascade reaction. To further substantiate the cooperative effect, an excess of pyridine was introduced into the $Pd(OAc)_2$ system. A greatly enhanced activity was observed, giving benzylidene malononitrile in a yield of 79% under identical reaction conditions; nonetheless, it is still lower than that obtained by Pd/COF-TpPa-Py (98%). Furthermore, Pd/POP-py afforded a product yield of 67%, which is also inferior to Pd/COF-TpPa-Py in terms of the reaction rate. Taking into account that these catalysts have similar amounts of catalytic components, the significant difference in the activities should be ascribed to different utilization efficiencies of these catalysts. In Pd/COF-TpPa-Py, the Pd metalated pyridine and free pyridine are site-isolated in the accessible ordered channel wall, thereby maximizing their utility, which leads to the high activity. In contrast, various catalytic related species dynamically exist in the homogeneous $Pd(OAc)_2$/pyridine catalytic system, thus compromising their efficiency. With respect to Pd/POP-py, some active sites may be buried due to their irregular pore structures.

In order to further illustrate the advantages of COFs for the design of efficient catalysts for cascade reactions, we compared the activities of Pd/COF-TpPa-Py and $Pd(OAc)_2$/pyridine at a higher substrate to catalyst ratio (the molar ratio of reagent to Pd, S/C = 250). To track the reaction pathway more directly, the one-pot cascade synthesis of benzylidene malononitrile from benzyl alcohol was performed for different reaction times. The difference in reactivity between the two catalytic systems was clearly manifested in the reaction kinetics. Time-dependent conversion curves indicated that Pd/COF-TpPa-Py was much faster than the homogeneous control in terms of turnover frequency. At 0.4 mol% catalyst loading (based on Pd species),

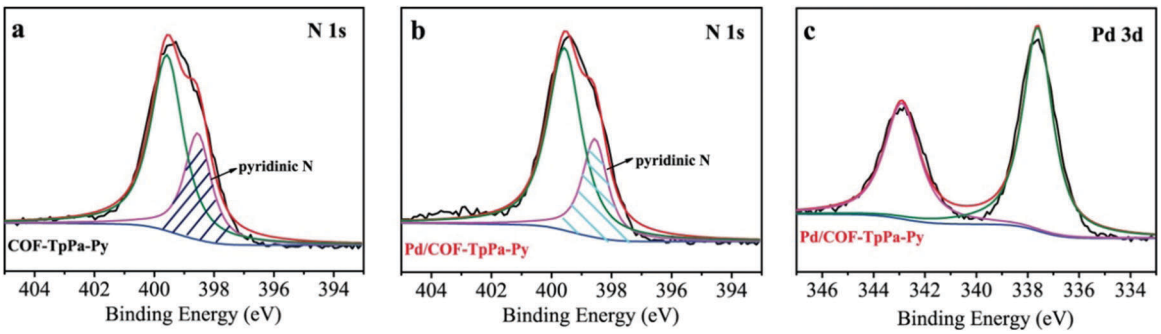

Fig. 2 N 1s and Pd 3d XPS spectra of COF-TpPa-Py and Pd/COF-TpPa-Py.

Published on 23 January 2017. Downloaded on 28/06/2017 16:16:36.

the oxidation of benzyl alcohol was completed within 16 h for Pd/COF-TpPa-Py. In the case of $Pd(OAc)_2$/pyridine, benzaldehyde was observed in a yield of 59% after 16 h and after prolonging the reaction time to 24 h, only a slightly increased conversion was obtained (67%). After introducing malononitrile into the reaction solution, the amount of intermediate benzaldehyde decreased rapidly to a low level, whereas the yield of benzylidene malononitrile increased sharply and leveled off at *ca.* 92% within 5 h for Pd/COF-TpPa-Py. In this step, Pd/COF-TpPa-Py is at least 2 times more active than the homogeneous control. These results revealed that Pd/COF-TpPa-Py exhibited superior performance in comparison with $Pd(OAc)_2$/pyridine, thus underscoring the great potential of COFs for the deployment of multifunctional catalysts for cascade catalysis (Fig. 3).

To identify if the catalysis occurs on the surface or within the pores, a relatively large size alcohol (cholesterol) was used as a reactant. Pd/COF-TpPa-Py afforded an 8% cholesterol conversion, while the homogeneous Pd/pyridine catalyst gave the corresponding oxide product in a yield as high as 87% under identical conditions, thus implying that cholesterol is too big to efficiently access the active sites anchored in the pores. These results reveal that most of the reactions occur in the pores (Table S1, ESI†).

Given that the recyclability of the catalyst is a crucial performance metric for cost-effective industrial processes, we investigated this property for Pd/COF-TpPa-Py. Analysis of the supernatant from the synthesis of benzylidene malononitrile by ICP-OES showed that the Pd species leaching was below the detection limit of 0.1 ppm. Moreover, it is observed that the catalyst could be recycled at least 6 times without a significant drop in the product yield (95% after 5 cycles), thus highlighting the heterogeneous nature of the catalytic process (Fig. 4). The robustness of the catalyst was further confirmed by the well-retained crystallinity and pore structure, and the chemical state of the Pd species in Pd/COF-TpPa-Py after the reaction as evidenced by XRD, N_2 adsorption and XPS spectroscopy, respectively (Fig. S10, ESI†).

Encouraged by the results described above, we extended the Pd/COF-TpPa-Py catalyzed one-pot cascade synthesis to other α,β-unsaturated dinitriles from alcohols, and the results are presented in Table 2. Primary benzylic alcohols were converted to the corresponding aldehydes in 92–96% yields (Table 2, entries 1–5) and then reacted with malononitrile to efficiently transform to the corresponding dinitriles. It is noteworthy that

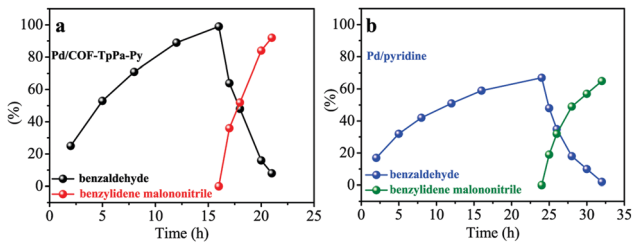

Fig. 3 Yield *versus* reaction time of the (a) Pd/COF-TpPa-Py and (b) Pd/pyridine catalysts for the one-pot cascade oxidation–Knoevenagel condensation reaction. Reaction conditions are similar to those given in Table 1 except for the S/C ratio and reaction time.

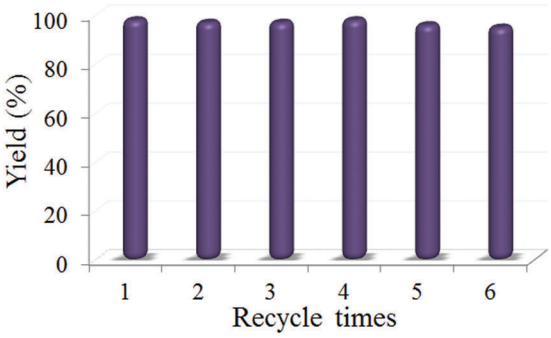

Fig. 4 Recycling tests of the Pd/COF-TpPa-Py in the cascade synthesis of benzylidene malononitrile from benzyl alcohol. Reaction conditions are the same as those given in Table 1.

Table 2 Pd/COF-TpPa-Py catalyzed cascade oxidation–Knoevenagel condensation reactions from alcohols to α,β-unsaturated dinitriles[a]

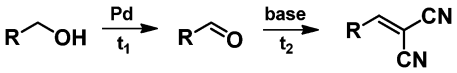

Entry	R	Time (h) $[t_1 + t_2]$	Conv. (%) *A*	Yield (%) *B*	Yield (%) *C*
1	4-CH_3O–C_6H_5	4 + 1.5	99	Trace	99
2	4-CH_3–C_6H_5	4 + 1.5	98	Trace	97
3	4-NO_2–C_6H_5	7 + 2	92	Trace	91
4	4-Cl–C_6H_5	6 + 2	96	Trace	94
5	3-Cl–C_6H_5	6 + 2	93	Trace	93
6	*n*-C_6H_{13}	12 + 5	91	Trace	91
7	*n*-C_8H_{17}	12 + 5	94	Trace	93

[a] Reaction conditions: a mixture of alcohol (1 mmol), toluene (10 mL), and Pd/COF-TpPa-Py was stirred at 80 °C under O_2 (1 atm) for t_1 h and then malononitrile (1.05 mmol) was introduced, and the reaction continued for t_2 h.

this catalytic system shows tolerance to a variety of substituents on aromatic nuclei. Aliphatic primary alcohols were oxidized to the aldehydes selectively and then to dinitriles, but they are relatively inert and thus required longer reaction times (Table 2, entries 6 and 7). To further extend the reaction scope, various methylene compounds instead of malononitrile were tested. When ethyl cyanoacetate was used, the cascade reaction can smoothly proceed, although more than threefold time is required to reach a similar final product yield (5 h, 97%) in comparison with employing malononitrile as a reagent in the Knoevenagel condensation step. However, when diethyl malonate was used, the second condensation step was suppressed greatly, which made the whole one-pot synthesis inefficient for production. Specifically, only 4% of benzaldehyde was observed to convert to diethyl 2-benzylidenemalonate after 8 h (Table S2, ESI†). Considering that the Knoevenagel condensation is a model reaction to evaluate the catalyst basicity, and Pd/COF-TpPa-Py can facilitate the Knoevenagel condensation between benzaldehyde and malononitrile or less active ethyl cyanoacetate, but not for relatively inert diethyl malonate, which is presumed to be catalyzed by strong base sites, therefore, the basicity of Pd/COF-TpPa-Py was evaluated to be moderately strong.

 This journal is © The Royal Society of Chemistry and the Chinese Chemical Society 2017

Published on 23 January 2017. Downloaded on 28/06/2017 16:16:36.

Conclusions

In summary, we have demonstrated the deployment of a chemically stable pyridine-based COF in a bifunctional catalyst after introducing Pd species by virtue of the base catalytic behavior and as a nitrogen donor to bind metal species of pyridine moieties. The resultant catalyst demonstrates excellent performance in the cascade oxidation–Knoevenagel condensation reaction from alcohols to α,β-unsaturated dinitriles. Due to the combined contributions of the ordered porous structure, highly accessible active sites, and the site isolated manner of the two catalytic components, Pd/COF-TpPa-Py far outperforms the corresponding homogeneous catalyst (Pd/pyridine) in terms of the turnover frequency. Our work therefore not only advances COFs as a new type of host material for the deployment of multifunctional catalysts, but also provides a new perspective for the design of highly efficient and robust heterogeneous catalysts for cascade catalysis. Studies aimed at designing new COF-based catalysts for advanced cascade catalysis applications are currently underway in our laboratory.

Acknowledgements

The authors acknowledge the University of South Florida the National Science Foundation (DMR-1352065) for financial support of this work.

Notes and references

1 (*a*) M. J. Climent, A. Corma, S. Iborra and M. J. Sabater, *ACS Catal.*, 2014, **4**, 870–891; (*b*) M. J. Climent, A. Corma and S. Iborra, *Chem. Rev.*, 2011, **111**, 1072–1133; (*c*) K. C. Nicolaou and J. S. Chen, *Chem. Soc. Rev.*, 2009, **38**, 2993–3009; (*d*) C. Grondal, M. Jeanty and D. Enders, *Nat. Chem.*, 2010, **2**, 167–178; (*e*) T. L. Lohr and T. J. Marks, *Nat. Chem.*, 2015, **7**, 477–482.

2 (*a*) J. C. Wasilke, S. J. Obrey, R. T. Baker and G. C. Bazan, *Chem. Rev.*, 2005, **105**, 1001–1020; (*b*) A. E. Fernandes, O. Riant, K. F. Jensen and A. M. Jonas, *Angew. Chem., Int. Ed.*, 2016, **55**, 11044–11048; (*c*) N. R. Shiju, A. H. Alberts, S. Khalid, D. R. Brown and G. Rothenberg, *Angew. Chem., Int. Ed.*, 2011, **50**, 9615–9619.

3 (*a*) A. Arnanz, M. Pintado-Sierra, A. Corma, M. Iglesias and F. Sánchez, *Adv. Synth. Catal.*, 2012, **354**, 1347–1355; (*b*) Y. Zhang, B. Li and S. Ma, *Chem. Commun.*, 2014, **50**, 8507–8510; (*c*) E. Merino, E. Verde-Sesto, E. M. Maya, M. Iglesias, E. Sánchez and A. Corma, *Chem. Mater.*, 2013, **25**, 981–988; (*d*) Y. Yang, X. Liu, X. Li, J. Zhao, S. Bai, J. Liu and Q. Yang, *Angew. Chem., Int. Ed.*, 2012, **124**, 9298–9302; (*e*) Y.-B. Huang, J. Liang, X.-S. Wang and R. Cao, *Chem. Soc. Rev.*, 2017, **46**, 126–157; (*f*) Y. Huang, S. Xu and V. S.-Y. Lin, *Angew. Chem., Int. Ed.*, 2011, **50**, 661–664; (*g*) K. K. Sharma and T. Asefa, *Angew. Chem., Int. Ed.*, 2005, **44**, 1826–1830.

4 (*a*) D.-Y. Hong, Y. K. Hwang, C. Serre, G. Férey and J.-S. Chang, *Adv. Funct. Mater.*, 2009, **19**, 1537–1552; (*b*) R. Srirambalaji, S. Hong, R. Natarajan, M. Yoon, R. Hota, Y. Kim, Y. H. Ko and K. Kim, *Chem. Commun.*, 2012, **48**, 11650–11652; (*c*) F. Vermoortele, R. Ameloot, A. Vimont, C. Serre and D. D. Vos, *Chem. Commun.*, 2011, **47**, 1521–1523; (*d*) Q. Han, B. Qi, W. Ren, C. He, J. Niu and C. Duan, *Nat. Commun.*, 2015, **6**, 10007; (*e*) T. Toyao, M. Fujiwaki, Y. Horiuchi and M. Matsuoka, *RSC Adv.*, 2013, **3**, 21582–21587; (*f*) A. Dhakshinamoorthy and H. Garcia, *ChemSusChem*, 2014, **7**, 2392–2410; (*g*) Y. Qi, Y. Luan, X. Peng, M. Yang, J. Hou and G. Wang, *Eur. J. Inorg. Chem.*, 2015, 5099–5105; (*h*) Y. Horiuchi, T. Toyao, M. Fujiwaki, S. Dorshi, T.-H. Kim and M. Matsuoka, *RSC Adv.*, 2015, **5**, 24687–24690; (*i*) Y.-Z. Chen, Y.-X. Zhou, H. Wang, J. Lu, T. Uchida, Q. Xu, S.-H. Yu and H.-L. Jiang, *ACS Catal.*, 2015, **5**, 2062–2069; (*j*) Z. Miao, Y. Luan, C. Qi and D. Ramella, *Dalton Trans.*, 2016, **45**, 13917–13924.

5 (*a*) K. M. Koeller and C. H. Wong, *Chem. Rev.*, 2000, **100**, 4465–4493; (*b*) H. Seong, H.-T. Chen, J. W. Wiench, M. Pruski and V. S.-Y. Lin, *Angew. Chem., Int. Ed.*, 2005, **44**, 1826–1830; (*c*) Á. G. Baribar, D. Reichert, C. Mügge, S. Seger, H. Gröger and R. Kourist, *Angew. Chem., Int. Ed.*, 2016, **55**, 14823–14827; (*d*) L. Chen, Y. Yang and D. Jiang, *J. Am. Chem. Soc.*, 2010, **132**, 9138–9143; (*e*) L. Chen, Y. Honsho, S. Seki and D. Jiang, *J. Am. Chem. Soc.*, 2010, **132**, 6742–6748.

6 (*a*) A. P. Côté, A. I. Benin, N. W. Ockwig, M. O'Keeffe, A. J. Matzger and O. M. Yaghi, *Science*, 2005, **310**, 1166–1170; (*b*) X. Feng, X. Ding and D. Jiang, *Chem. Soc. Rev.*, 2012, **41**, 6010–6022; (*c*) S.-Y. Ding and W. Wang, *Chem. Soc. Rev.*, 2013, **42**, 548–568; (*d*) L. Ascherl, T. Sick, J. T. Margraf, S. H. Lapidus, M. Calik, C. Hettstedt, K. Karaghiosoff, M. Döblinger, T. Clark, K. W. Chapman, F. Auras and T. Bein, *Nat. Chem.*, 2016, **8**, 310–316; (*e*) D. N. Bunck and W. R. Dichtel, *Angew. Chem., Int. Ed.*, 2012, **51**, 1885–1889; (*f*) Y. Zeng, R. Zou, Z. Luo, H. Zhang, X. Yao, X. Ma, R. Zou and Y. Zhao, *J. Am. Chem. Soc.*, 2015, **137**, 1020–1023; (*g*) Z.-F. Pang, S.-Q. Xu, T.-Y. Zhou, R.-R. Liang, T.-G. Zhan and X. Zhao, *J. Am. Chem. Soc.*, 2016, **138**, 4710–4713; (*h*) S. Chandra, S. Kandambeth, B. P. Biswal, B. Lukose, S. M. Kunjir, M. Chaudhary, R. Babarao, T. Heine and R. Banerjee, *J. Am. Chem. Soc.*, 2013, **135**, 17853–17861.

7 (*a*) S.-Y. Ding, M. Dong, Y.-W. Wang, Y.-T. Chen, H.-Z. Wang, C.-Y. Su and W. Wang, *J. Am. Chem. Soc.*, 2016, **138**, 3031–3037; (*b*) C. J. Doonan, D. J. Tranchemontagne, T. G. Glover, J. R. Hunt and O. M. Yaghi, *Nat. Chem.*, 2010, **2**, 235–238; (*c*) Y. Zeng, R. Zou and Y. Zhao, *Adv. Mater.*, 2016, **28**, 2855–2873.

8 (*a*) H. Xu, J. Gao and D. Jiang, *Nat. Chem.*, 2015, **7**, 905–912; (*b*) Q. Fang, S. Gu, J. Zheng, Z. Zhuang, S. Qiu and Y. Yan, *Angew. Chem., Int. Ed.*, 2014, **53**, 2878–2882; (*c*) S.-Y. Ding, J. Gao, Q. Wang, Y. Zhang, W.-G. Song, C.-Y. Su and W. Wang, *J. Am. Chem. Soc.*, 2011, **133**, 19816–19822; (*d*) Y. Peng, Z. Hu, Y. Gao, D. Yuan, Z. Kang, Y. Qian, N. Yan and D. Zhao, *ChemSusChem*, 2015, **8**, 3208–3212; (*e*) H. B. Aiyappa, J. Thote, D. B. Shinde, R. Banerjee and S. Kurungot, *Chem. Mater.*, 2016, **28**, 4375–4379; (*f*) V. S. Vyas, F. Haase, L. Stegbauer, G. Savasci, F. Podjaski, C. Ochsenfeld and B. V. Lotsch, *Nat. Commun.*, 2015, **6**, 8508; (*g*) S. Lin, C. S. Diercks, Y.-B. Zhang,

N. Kornienko, E. M. Nichols, Y. Zhao, A. R. Paris, D. Kim, P. Yang, O. M. Yaghi and C. J. Chang, *Science*, 2015, **349**, 1208–1213; (*h*) X. Wang, X. Han, J. Zhang, X. Wu, Y. Liu and Y. Cui, *J. Am. Chem. Soc.*, 2016, **138**, 12332–12335; (*i*) Q. Sun, B. Aguila, J. A. Perman, N. Nguyen and S. Ma, *J. Am. Chem. Soc.*, 2016, **138**, 15790–15796.

9 (*a*) H. Ma, B. Liu, B. Li, L. Zhang, Y.-G. Li, H.-Q. Tan, H.-Y. Zang and G. Zhu, *J. Am. Chem. Soc.*, 2016, **138**, 5897–5903; (*b*) H. Xu, S. Tao and D. Jiang, *Nat. Mater.*, 2016, DOI: 10.1038/nmat4611.

10 (*a*) S. Mitra, S. Kandambeth, B. P. Biswal, M. A. Khayum, C. K. Choudhury, M. Mehta, G. Kaur, S. Banerjee, A. Prabhune, S. Verma, S. Roy, U. K. Kharul and R. Banerjee, *J. Am. Chem. Soc.*, 2016, **138**, 2823–2828; (*b*) Y. Du, H. Yang, J. M. Whiteley, S. Wan, Y. Jin, S.-H. Lee and W. Zhang, *Angew. Chem., Int. Ed.*, 2016, **55**, 1737–1741; (*c*) G. H. V. Bertrand, V. K. Michaelis, T.-C. Ong, R. G. Griffin and M. Dincă, *Proc. Natl. Acad. Sci. U. S. A.*, 2013, **110**, 4923–4928.

11 Y.-L. Zhang, S. Liu, S. Liu, F. Liu, H. Zhang, Y. He and F.-S. Xiao, *Catal. Commun.*, 2011, **12**, 1212–1217.

12 S. Kandambeth, A. Mallick, B. Lukose, M. V. Mane, T. Heine and R. Banerjee, *J. Am. Chem. Soc.*, 2012, **134**, 19524–19527.

13 (*a*) T. Iwasawa, M. Tokunaga, Y. Obora and Y. Tsuji, *J. Am. Chem. Soc.*, 2004, **126**, 6554–6555; (*b*) T. Nishimura, T. Onoue, K. Ohe and S. Uemura, *J. Org. Chem.*, 1999, **64**, 6750–6755.

14 S. Chandra, T. Kundu, K. Dey, M. Addicoat, T. Heine and R. Banerjee, *Chem. Mater.*, 2016, **28**, 1489–1494.

15 H. Yang, X. Han, G. Li and Y. Wang, *Green Chem.*, 2009, **11**, 1184–1193.

Published on 23 January 2017. Downloaded on 28/06/2017 16:16:36.

 This journal is © The Royal Society of Chemistry and the Chinese Chemical Society 2017